OncoTargets and Therapy

Dovepress

open access to scientific and medical research

Open Access Full Text Article

ORIGINAL RESEARCH

RETRACTED ARTICLE: Hsa_circ_RNA_0011780 Represses the Proliferation and Metastasis of Non-Small Cell Lung Cancer by Decreasing FBXW7 via Targeting miR-544a

This article was published in the following Dove Press journal:
OncoTargets and Therapy

Yong Liu[1,*]
Chuanping Yang[2,*]
Chengsong Cao[1]
Qing Li[1]
Xin Jin[1]
Hanping Shi[3–5]

[1]Department of Oncology, Xuzhou Central Hospital, Xuzhou School of Clinical Medicine, Nanjing Medical University, Xuzhou 221000, People's Republic of China; [2]Department of Thoracic Surgery, Xuzhou Central Hospital, Xuzhou School of Clinical Medicine, Nanjing Medical University, Xuzhou 221000, People's Republic of China; [3]Department of Gastrointestinal Surgery/Department of Clinical Nutrition, Beijing Shijitan Hospital, Capital Medical University, Beijing 100038, People's Republic of China; [4]Department of Oncology, Capital Medical University, Beijing 100069, People's Republic of China; [5]Beijing International Science and Technology Cooperation Base of Tumor Metabolism and Nutrition, Beijing 100038, People's Republic of China

*These authors contributed equally to this work

Purpose: Circular RNA (circRNA) is involved in the development of various cancers. However, whether circRNA can inhibit the tumorigenesis of non-small cell lung cancer (NSCLC) is still unclear. We aimed to explore the epigenetic function of tumor-suppressive circRNA (hsa_circ_RNA_0011780) and its downstream regulatory factors in NSCLC.

Patients and Methods: Quantitative polymerase chain reaction (qPCR) was used to evaluate hsa_circ_11780 expression in NSCLC tissues and cell lines. The impact of high hsa_circ_11780 expression on overall survival in patients with NSCLC was tested using the Log rank test. The association between decreased hsa_circ_11780 expression and clinicopathological features in patients with NSCLC was analyzed using the Chi-squared test. In vitro cell proliferation and apoptosis were assayed using the cell counting kit-8 (CCK-8) and flow cytometry, respectively. Mice xenograft models were used to determine the tumor promoting effects of hsa_circ_11780 on NSCLC in vivo. The underlying regulatory mechanism was predicted using bioinformatics and verified by a dual-luciferase reporter assay, RNA transfection, qPCR, and Western blotting. The correlation between miR-544a and hsa_circ_11780 expression was verified using Spearman correlation coefficient.

Results: The expression of hsa_circ_11780 in NSCLC tissues and cell lines strongly declined. Low hsa_circ_11780 expression is more likely to present in patients with a large tumor size (>3cm), distant metastasis, and poor overall survival. hsa_circ_11780 overexpression strongly inhibited proliferation, migration, and invasion of NSCLC cells (H226 and A549) in vitro and inhibited tumor growth in vivo. Furthermore, hsa_circ_11780 repressed miR-544a function by competitively binding to the complementary sites of miR-544a. miR-544a released by the declining expression of hsa_circ_11780 reduced the protein concentration of F-Box and WD repeat domain containing 7 (FBXW7) in NSCLC cells.

Conclusion: FBXW7 expression mediated by the hsa_circ_11780/miR-544a axis is markedly associated with the proliferation, migration, and invasion of NSCLC, resulting in decreased survival. These findings suggest that this regulatory axis may serve as a novel therapeutic target in NSCLC.

Keywords: non-small cell lung cancer, hsa_circ_11780, F-box and WD repeat domain containing 7, miR-544a, proliferation, metastasis

Introduction

Lung cancer ranks first in both cancer incidence and cancer-related mortality globally.[1] Two histological subtypes, adenocarcinoma (51%) and squamous cell carcinoma (30%), mainly constitute non-small cell lung cancer (NSCLC), representing 85% of all lung cancers.[2] Clinically, NSCLC is usually diagnosed in the late stages of disease

Correspondence: Hanping Shi
Fax +86-0951-6743244
Email shihanpingbj@126.com

submit your manuscript | www.dovepress.com
DovePress
http://doi.org/10.2147/OTT.S236162

development,[3] leading to a lack of treatment options and poor prognosis.[4] Although approximately 30% of patients with advanced NSCLC initially respond to chemotherapy and radiotherapy, many experience relapse or metastasis occurrence within 6 to 12 months of treatment. Elevated cell proliferation is common in tumorigenesis and is associated with high recurrence rates and treatment resistance in patients with NSCLC. Genetic studies of the aberrant expression underlying NSCLC development will help us fully understand the tumorigenesis of NSCLC, leading to the identification of promising therapeutic targets that may ameliorate the poor survival rates of patients.

Due to advances in sequencing technology, non-coding RNAs (ncRNAs) are being increasingly identified to be involved in the development of disease.[5,6] circRNA is an ncRNA with a covalently closed loop that does not have a 5′ cap or 3′ polyadenylation tail.[7] Studies have shown that circRNA can affect the multiple functions of tumor cells and can be used as a helpful predictor for tumor prognosis.[8] Chen et al reported that circPTN promoted proliferation and maintained stem cell characteristics of glioma cells by increasing SOX9/ITGA5 concentrations by targeting miR-145-5p.[9] The hsa_circ_0035483/miR-335/CCNB1 axis in renal clear cell carcinoma not only promoted autophagy and tumor growth, but also enhanced gemcitabine resistance in tumor cells.[10] In addition, circDENND4C accelerated glycolysis, migration and invasion of breast cancer cells under hypoxia by competitively sponging miR-200b/200c.[11] Growing evidence suggests that circRNA promotes various biological behaviors in the development of NSCLC, including proliferation,[12] invasion,[13] migration,[13] and chemoresistance.[14] Therefore, studying the important role of circRNA in tumorigenesis may be effective for identifying novel molecular targets to help inhibit the development of NSCLC.

An increasing number of circRNAs have been found to be involved in NSCLC, although few have been found to function as tumor suppressors. In our investigation, we found hsa_circ_11780 (named consistently with that stated in the circBase ID, http://www.circbase.org) was upregulated in the adjacent tissue rather than in the NSCLC cancerous tissue. hsa_circ_11780, located at chromosome 1:39749737–39793025, can transcribe the mRNA of microfilament microtubule cross-link factor 1 (MACF1). The data from our study identified that hsa_circ_11780 inhibited proliferation, migration, and invasion of NSCLC. This indicates that hsa_circ_11780 acts as a tumor suppressor. Developing a molecular intervention targeting hsa_circ_11780 and the relevant downstream pathway, could serve as an effective molecular target for improving the prognosis of patients with NSCLC.

Materials and Methods

Patients, Corresponding Tissues and Follow-Up

Totally 93 NSCLC patients, who received no radiotherapy or chemotherapy before hospitalization, were enrolled at the Xuzhou Central Hospital (Xuzhou, Jiangsu, China) from April 2014 to October 2014. All patients were diagnosed by pathology. All corresponding tissues were acquired by biopsy (bronchofiberscope and fine-needle aspiration) or surgery. All subsequent tissues were all rapidly frozen at −80 °C. 5-year follow-up was implemented to attain overall survival. The study was approved by the Ethics Committee of XuZhou Central Hospital. Written informed consent was received from all patients before this study.

RNA Extraction and Quantitative PCR

Based on the manufacturer's protocol, total RNA was extracted from tissues and cultured cells using Trizol solution (Thermo Fisher Scientific, Waltham, MA, USA). Total RNA was transcribed to cDNA using SuperScript IV Reverse Transcript (Thermo Fisher Scientific, Waltham, MA, USA). The prepared cDNA was measured by a NanoDrop 2000 spectrophotometer (Thermo Fisher Scientific, Waltham, MA, USA). Then, in accordance with the protocol of kit, quantitative PCR for target RNA in tissues and cells was performed using PowerUp™ SYBR™ Green Master Mix (Thermo Fisher Scientific, Waltham, MA, USA) in a 96-well PCR plate on the Applied Biosystems 7500 Sequence Detection system. All expression of target RNA was calculated using the $2^{-\Delta\Delta}$ Ct method with glyceraldehyde-phosphate dehydrogenase (GAPDH) as the endogenous control. All primer sequences this study used are presented in Supplementary Table SI.

Cell Culture

RPMI (Roswell Park Memorial Institute) 1640 Medium (Gibco, Thermo Fisher Scientific, Waltham, MA, USA) supplemented with 10% fetal bovine serum (Gibco, Thermo Fisher Scientific, Waltham, MA, USA) was used to culture H226, H520, SK-MES-1, A549, H1975, H1299 and normal human bronchial epithelium cell line BEAS-2B. All of them were in an atmosphere with 5% CO^2 at

37 °C, purchased from the Chinese Academy of Sciences (Shanghai Institute of Cell Biology, Shanghai, China).

Gene Overexpression and Cells Transfection

For gene overexpression, lentiviral vectors (pcD-ciR vector, Geenseed Biotech, Guangzhou, China) were used to construct hsa_circ_11780 expressing particles (oe- hsa_circ_11780, hsa_circ_11780 sequence was shown in Supplemental Table SI). Hsa_circ_11780-cDNA or NC-cDNA (MOI = 20) with polybrene was transfected into H226 and A549. 24h after transfection, a fresh medium replacement was done to the culture medium. Stably transfected cells were selected by puromycin (1 μg/mL). The Puromycin (1 μg/mL, 2–3 times) selection was done until green fluorescence was shown in all cancer cells via the fluorescence microscope (Olympus IX71, Japan).

Proliferation Ability of NSCLC Cells

NSCLC cells were cultured in 96-well plates (2×10^4 cells/well) for 5 days. Cell viability was measured every 24h using Cell Counting Kit-8 (CCK-8; Medchembio, USA) according to the manufacturer's instruction. The tested absorbance at each day was collected to calculate the proliferation curves.

Migration Ability and Invasion Ability in NSCLC Cells

Transwell inserts with a polycarbonate membrane (8.0μm pores; Corning, New York, NY, USA) were applied for migration assays. Membranes were additionally coated with Matrigel matrix (BD Biosciences, Franklin, NJ, USA) for invasion assays. After NSCLC was transfected with the expression vector or the vector control 24 hrs later, 200μL medium with tumor cells (5×10^5) was seeded in the upper chamber, while 600μL medium supplemented 10% fetal bovine serum was added in the lower chamber. Following incubation for 24h (37 °C in a 5% CO_2), the cells on the upper surface of the polycarbonate membrane were removed. The cells attached to the bottom of the membrane were defined as migrated or invaded. All of those cells were fixed, stained, being counted by the microscope (Leica DM20, Leica Microsystems Inc, Buffalo Grove, IL, USA)

Apoptosis Assay by Flow Cytometry

After 48h culture, the apoptosis analysis of NSCLC cells with oe-NC or oe-Circ was analyzed by the Apoptosis Detection Kits (eBiosciences, Waltham, MA, USA). Antibodies with Annexin V/FITC were incubated with tumor cells (5×10^4 cell) for 30 min. Cells were measured by FACS Calibur Flow Cytometry (BD Biosciences, Franklin, NJ, USA).

Animal Experiment and Tumor Growth in vivo

The animal experiments were approved by the Institutional Animal Ethics Committee of Xuzhou Central Hospital. All the procedures of animal experiments were performed in strict accordance with the Laboratory Animal protection, welfare and ethics rules of the Institutional Animal Ethics Committee of Xuzhou Central Hospital. 4-week-old BALB/c-nude mice were purchased from the Laboratory Animal Center of Xuzhou School of Clinical Medicine, fed in an atmosphere with a 12h light/dark cycle under specific pathogen-free conditions. NSCLC cells (2×10^5 cells in 100μL) transfected with an expression vector (oe-hsa_circ_11780) or vector control (oe-NC) were respectively incubated subcutaneously into mice (each group n = 5). The tumor sizes of every mouse were collected every week. In the fifth week, tumor weight was measured after the mice were sacrificed.

Dual-Luciferase Reporter Analysis

The wildtype target lncRNA or the one containing a mutant miRNA- binding area were constructed (Invitrogen, Waltham, MA, USA). Both of these lncRNA were cloned with a luciferase gene in reporter vectors (Promega, Madison, WI, USA). The synthetic vectors, Renilla luciferase reporter vector, and miRNA mimic were co-transfected into cells using the Lipofectamine 2000 kit (Thermo Fisher Scientific, Waltham, MA, USA) following the protocol provided by the manufacturer, 48h later cells were seeded into 96-well plates. The luciferase activity of Renilla plasmid (as the endogenic control, Promega, Madison, WI, USA) and target gene was assessed via Dual-Luciferase Reporter Assay Kit (Promega, Madison, WI, USA).

RNA Binding Protein Immunoprecipitation Assay (RIP)

The Imprint® RNA Immunoprecipitation RIP Kit (Sigma-Aldrich, St. Louis, MO, USA) was used to analyze the interaction between hsa_circ_11780 and miR-544a according to the manufacturer's instruction. Briefly, H226 and A549 cells transfected with miR-544a mimics or miR-NC were cultured 48 h before anti-AGO2 RIP assay. After the

tumor cells were lysed by the lysis buffer (RNase inhibitor and protease inhibitor), the suspension was incubated with magnetic beads (conjugated with Ago2 antibody) (Abcam, San Francisco, CA, USA), or negative control IgG. Finally, the antibody binding RNA was identified by RIP-qPCR assay using the respective target primers.

Western Blotting Assay

NSCLC cells were resolved by RIPA buffer with 1 mmol/L protease inhibitors. A Bicinchoninic acid (BCA) Protein Assay Kit (Beyotime, Shanghai, China) was applied to measure the concentration of the protein samples in according with the manufacturer's guidance. The proteins were separated by 10% sodium dodecyl sulfate-polyacrylamide gel electrophoresis (SDS-PAGE), transfected to a nitrocellulose polyvinylidene Fluoride (PVDF) membrane (Bioss Antibodies, Beijing, China). PVDF membrane with primary antibodies (anti-FBWX7, 1:2000; Abcam, ab109617, San Francisco, CA, USA) was incubated at 4 °C overnight, using GAPDH (1:4000; Abcam, San Francisco, CA, USA) as the endogenous reference. Then the target blot on the membrane was incubated with the secondary antibody with horseradish peroxidase (HRP, 1:8000 dilution, Santa Cruz, CA, USA). The Western blot band was photographed by a chemiluminescence detection system (ECLTM, Pierce, Waltham, MA, USA), quantified by Image J software.

Statistics Analysis

All data were analyzed using GraphPad Prism 6 software (San Diego, CA, USA), and presented as the mean ± standard deviation. Comparison between two groups was carried out by Student's *t*-test. And the correlation between hsa_circ_11780 and miR-544a expression was evaluated via Spearman correlation coefficient. Each experiment was done independently three times. $p < 0.05$ was defined as a significant difference.

Results

Hsa_circ_11780 Expression Is Highly Related to Superior Survival in NSCLC

By analyzing a microarray dataset (GSE62182) in the Public Database (27 pairs of cancer tissues and adjacent normal tissues), we found hsa_circ_11780 declined the most in NSCLC tissues relative to adjacent normal tissues (Figure 1A). hsa_circ_11780 expression in 93 patients'

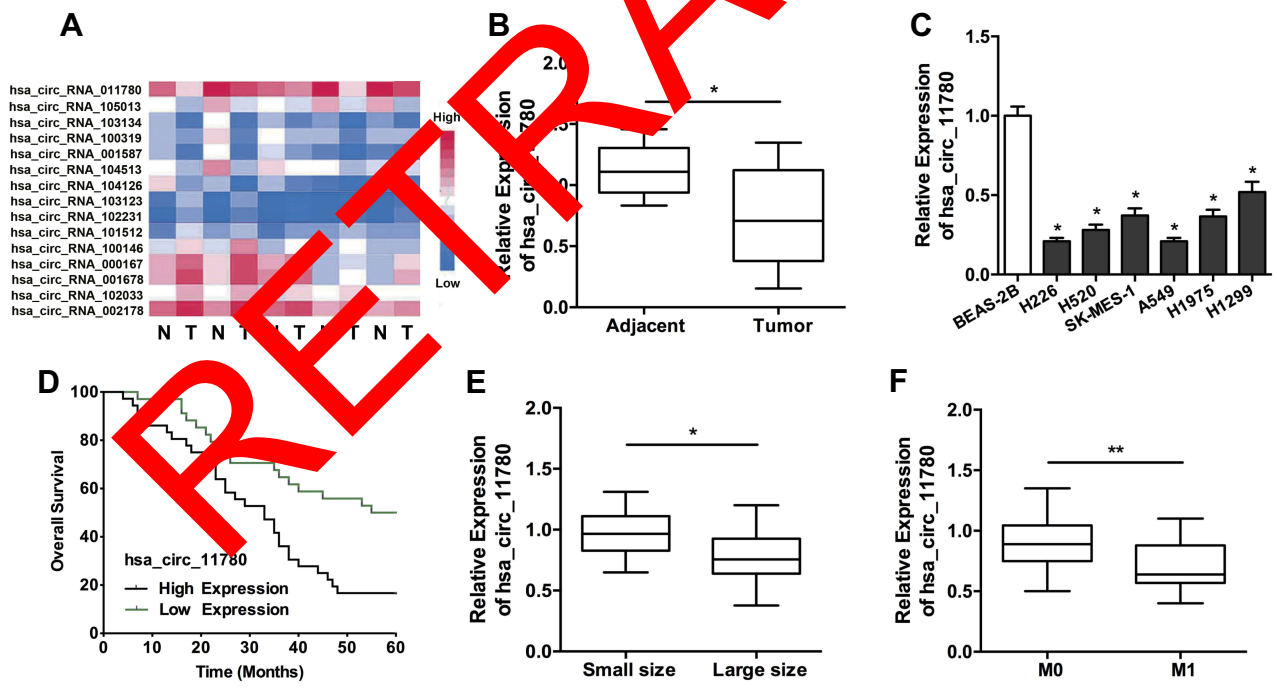

Figure 1 Hsa_circ_11780 expression is highly related to superior survival in NSCLC. (**A**) The heat map for differentially expressing circRNAs in NSCLC tissues compared to corresponding adjacent normal tissues based on circRNA mircoarray from the publish database (GSE62182). N for adjacent normal tissues; T for NSCLC tissues. (**B**) Expression of hsa_circ_11780 in NSCLC tissues and adjacent normal tissues shown by qPCR. (**C**) Hsa_circ_11780 expression in NSCLC cells (H226, H520, SK-MES-1, A549, H1975, and H1299) and BEAS-2B cells. (**D**) Overall survival of NSCLC patients with high and low Hsa_circ_11780 expression. (**E**) Expression of hsa_circ_11780 in NSCLC tissues with different tumor sizes (Small, n = 39; Large n = 54). (**F**) Expression of hsa_circ_11780 in NSCLC tissues with different M stage (M0, n = 55; M1 n = 38). $^{**}p < 0.01$, $^{*}p < 0.05$ compared to the control group.

tissues (tumor and adjacent normal tissues) was quantified using quantitative reverse transcriptase-polymerase chain reaction (qPCR), to verify the critical role of hsa_circ_11780 in NSCLC development. hsa_circ_11780 expression in NSCLC tissues was lower than that in adjacent normal tissues (Figure 1B, $p < 0.01$). Additionally, compared to a normal human bronchial epithelial cell line (BEAS-2B), hsa_circ_11780 expression was significantly decreased in NSCLC cells (H226, H520, SK-MES-1, A549, H1975, and H1299) (Figure 1C, $p < 0.01$). Patients with NSCLC were divided into two groups based on the median expression of hsa_circ_11780 (high group, n = 46; low group, n = 47). Clinicopathological analysis (Table 1) revealed that the decline in hsa_circ_11780 expression was significantly related to large tumor size (> 3 cm) ($p = 0.026$), distant metastasis ($p = 0.028$), and advanced TNM stage ($p = 0.023$). Based on Kaplan-Meier analysis, a lower expression of hsa_circ_11780 was associated with inferior overall survival (Figure 1D, $p < 0.05$). Moreover, after further stratification, the data showed that NSCLC patients with larger tumor nude (≥3cm) exhibited a higher decrease in hsa_circ_11780 expression than those patients with tumor ≤ 3cm (Figure 1E, $p < 0.01$). Expression of hsa_circ_11780 was lower in patients with M1 stage than in patients with M0 stage NSCLC (Figure 1F, $p < 0.01$). Altogether, our results indicated that hsa_circ_11780 is downregulated in NSCLC tissues, and it demonstrates a tumor-suppressive role in NSCLC.

Table 1 Relation Between Hsa_circ_11780 Expression and Clinicopathological Features in NSCLC (n = 93)

	Total n	Hsa_circ_11780 Expression		*P*-value
		Low n = 47	High n = 46	
Gender				0.602
Male	45	24	21	
Female	48	23	25	
Age				0.611
≤60	40	19	21	
>60	53	28	25	
Tumor size				0.026*
≤3 cm	39	25	14	
>3 cm	54	22	32	
Lymph node				0.105
Negative	36	22	14	
Positive	57	25	32	
Distant metastasis				0.028*
No	55	33	22	
Yes	38	14	24	
TNM stage				0.023*
I+II	35	23	12	
III+IV	58	24	34	
Pathology				0.349
Squamous carcinoma	48	22	26	
Adenocarcinoma	45	25	20	

Note: *$p < 0.05$ represents statistical difference.

Hsa_circ_11780 Restrains NSCLC Cell Proliferation, Migration, and Invasion in vitro

To confirm the influence of hsa_circ_11780 on the biological behavior of tumor cells, the expression of hsa_circ_11780 in two cell lines (A549 and H226) was increased by a synthesized lentiviral hsa_circ_11780-overexpressing (oe-circ) vector. Quantitative PCR was used to validate overexpression efficiency 48 h after transfection (Figure 2A, $p < 0.01$). Cell proliferation, measured by CCK8 in NSCLC, was repressed in cells overexpressing hsa_circ_11780 (Figure 2B and C $p < 0.05$). Moreover, the percentage of apoptotic cells (Figure 2D, $p < 0.05$) increased, while the migration and invasion of tumor cells (Figure 2E and F, $p < 0.05$) decreased after the expression of hsa_circ_11780 increased. Therefore, these data suggest that hsa_circ_11780 can mediate the malignant properties (proliferation, migration, and invasion) of NSCLC cells in vitro.

Hsa_circ_11780 Limits NSCLC Tumor Growth in vivo

A549 and H226 cells transfected with oe-circ or oe-NC were inoculated into immune-deficient mice to induce a xenograft tumor model. The results revealed that increased hsa_circ_11780 limited the growth (tumor size, Figure 3A and B, $p < 0.05$; tumor weight, Figure 3C and D, $p < 0.05$) of NSCLC tumor nodes, compared to that in vector-control mice. The macroscopic observation of tumor nodes is shown in Figure 3E and F. These results suggest that hsa_circ_11780 dysregulation is involved in NSCLC tumor formation in vivo.

Hsa_circ_11780 Modulates NSCLC Growth by Targeting miR-544a

circRNAs can upregulate target genes by endogenously competing with microRNA (miRNA). Bioinformatics analyses

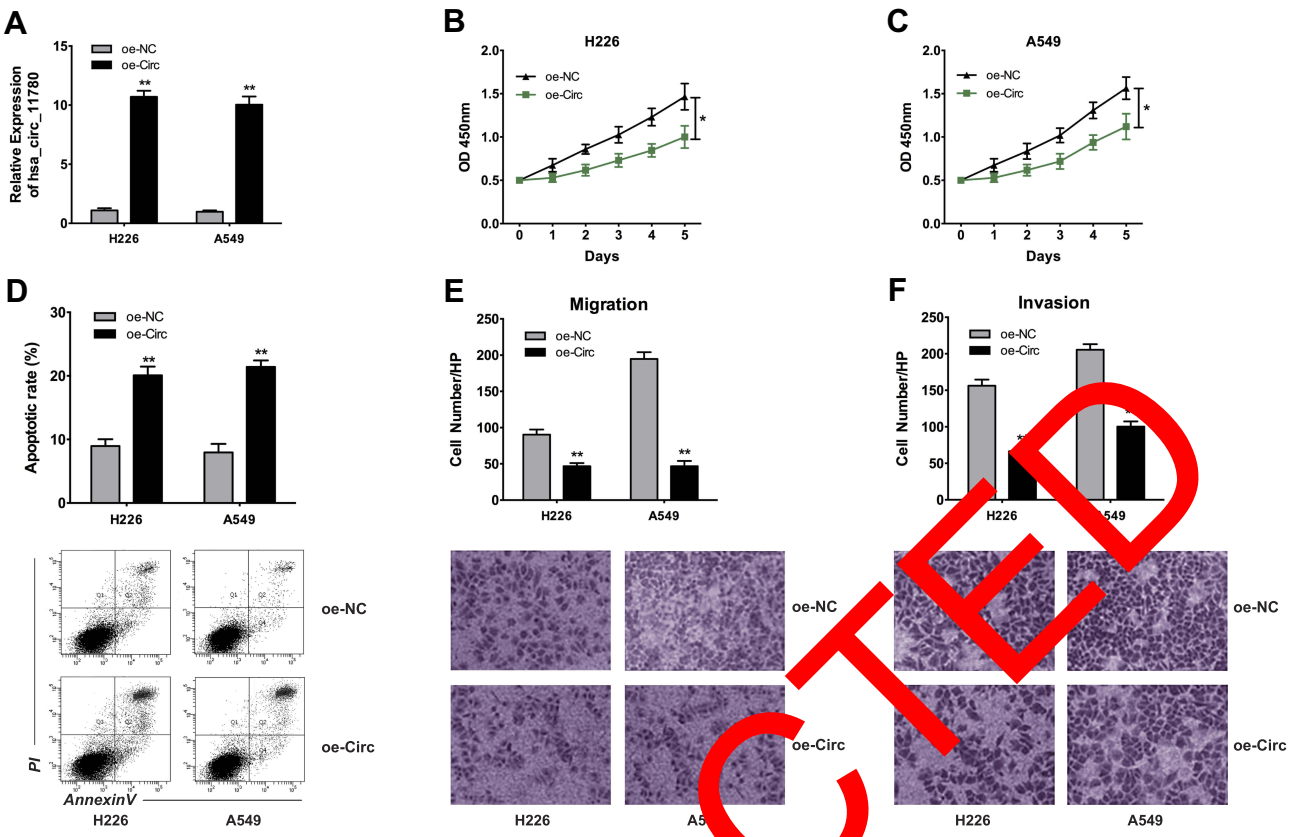

Figure 2 Hsa_circ_11780 restrains NSCLC cell proliferation, migration, and invasion in vitro. (**A**) Hsa_circ_11780 expression was increased by lentiviral vectors in NSCLC cells. (**B, C**) Proliferative ability of NSCLC cells transfected with overexpressing vector or vector control measured by CCK-8 test. (**D**) Flow cytometry showed the apoptotic rate of NSCLC cells transfected with overexpressing vector or vector control. (**E**) Migration ability of NSCLC cells after hsa_circ_11780 overexpression. (**F**) Invasion ability of NSCLC cells transfected with overexpressing vector or control. $^{**}p < 0.01$, $^{*}p < 0.05$ compared to the control group.

predicted that complementary base within miR-544a may be the direct target for hsa_circ_11780 (Figure 4A). Furthermore, assays validated that the luciferase activity of miR-544a was significantly repressed by the wild type hsa_circ_11780 rather than the mutant form (Figure 4B and C, $p<0.01$). Based on an immunoprecipitation assay carried out on NSCLC cells, we also verified that hsa_circ_11780 directly targeted miR-544a (Figure 4D and E, $p<0.01$). Additionally, the expression of miR-544a declined in NSCLC cells transfected with oe-hsa_circ_11780, compared to the oe-NC treated cells (Figure 4F, $p<0.01$). The expression of miR-544a was higher in NSCLC cells (H226, H520, SK-MES-1, A549, H1975, and H1299) than in BEAS-2B (Figure 4G, $p<0.01$). Similarly, miR-544a expression in NSCLC tissues was higher than that in adjacent normal tissues (Figure 4H, $p < 0.01$). A negative correlation between hsa_circ_11780 and miR-544a expression levels was found in human NSCLC tissue (Figure 4I, $R2 = -0.4291$, $p < 0.0001$). Collectively, our data suggested that hsa_circ_11780 interacted with miR-544a as a competing endogenous RNA to inhibit their action.

miR-544a Directly Targets FBWX7 in NSCLC Development

Based on bioinformatics analysis using TargetScan, we predicted that FBWX7, which exhibited decreased expression in NSCLC, maybe a downstream target for miR-544a. Their complementary binding relationship (Figure 5A) was verified by a luciferase reporter assay (Figure 5B and C, $p<0.01$). FBWX7 expression was strongly decreased by miR-544a inhibition in cancer cells transfected with oe-circ, compared to that in vector controls (Figure 5D and E, $p<0.01$). Therefore, these results indicate that FBWX7 is an effector protein targeted by the hsa_circ_11780/miR-544a axis in NSCLC.

Discussion

circRNA plays a significant role in numerous physiological processes and pathological progression.[15] Accumulating evidence has confirmed that aberrant expression of circRNA is associated with specific diseases. Abnormally high expression often results in malignant behavior of cancer cells, such as

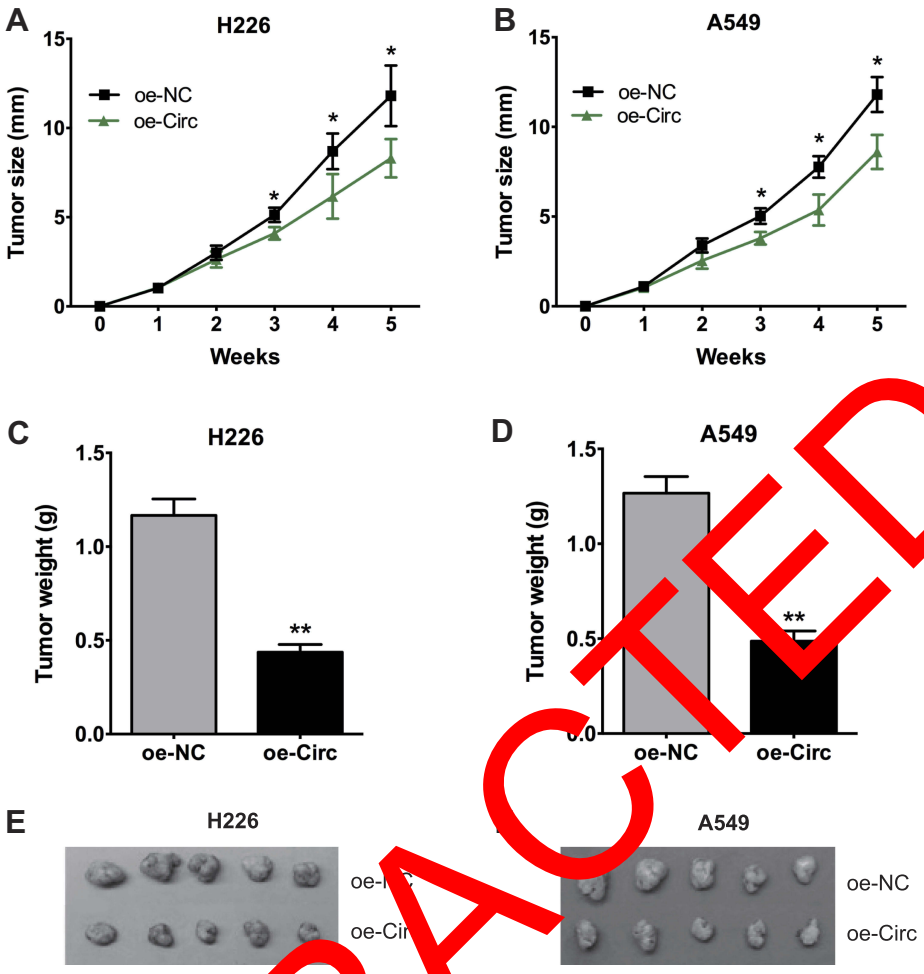

Figure 3 Hsa_circ_11780 limits NSCLC tumor growth in vivo. (**A, B**) Tumor size between hsa_circ_11780 overexpressing mice and the control mice. (**C, D**) Tumor weight of tumor nudes after stable overexpression of hsa_circ_11780. (**E**) Macroscopic observation of tumor nudes. $^{**}p < 0.01$, $^{*}p < 0.05$ compared to the control group.

proliferation, metastasis, and therapeutic resistance.[15] However, low expression of circRNAs in tumor tissues (compared to adjacent tissues), and its repressing effect on tumors, has been rarely studied. Researchers have reported that low-expression of circRNAs plays a role in tumor suppression, including lung cancer,[16] colorectal cancer,[17] hepatocellular carcinoma,[18] and breast cancer.[19] circRNA in these diseases can inhibit various pathological processes involved in cancer development, including apoptosis, proliferation, and invasion.[20] In the current study, we identified a novel circRNA named hsa_circ_11780, whose linear-form-mRNA can translate the protein MACF1. We revealed that decreased has_circ_11780 in cancerous tissue, was significantly involved in the proliferation and growth of NSCLC cells both in vitro and in vivo (Figures 2 and 3). In addition, we found that lower hsa_circ_11780 expression was a significant indicator for metastasis and poor prognosis of NSCLC (Table 1 & Figure 1). Next, we performed a migration and invasion assay in tumor cells and verified the suppressive effect of hsa_circ_11780 (Figure 2). Collectively, our results revealed that hsa_circ_11780 is a promising suppressor for distant metastasis and an indicator of poor survival in patients with NSCLC.

Sponging target miRNAs, for post-transcriptional regulation by competitively binding, is a functional property of circRNAs.[21] In our study, we applied bioinformatics analysis to predict the interaction between the hsa_circ_11780 and miR-544a (Figure 4A). The luciferase activity of the miR-544a was inhibited by wild-type hsa_circ_11780 but was not inhibited by the mutant form, thus demonstrating the direct-binding between them (Figure 4B and C). Furthermore, our results showed that hsa_circ_11780 overexpression suppressed the expression of miR-544a in tumor cells (Figure 5D). Therefore, since hsa_circ_11780 displayed a tumor-suppressive role and competitive repression of miR-544a, it is clear that miR- miR-544a acts as a significant oncogene for

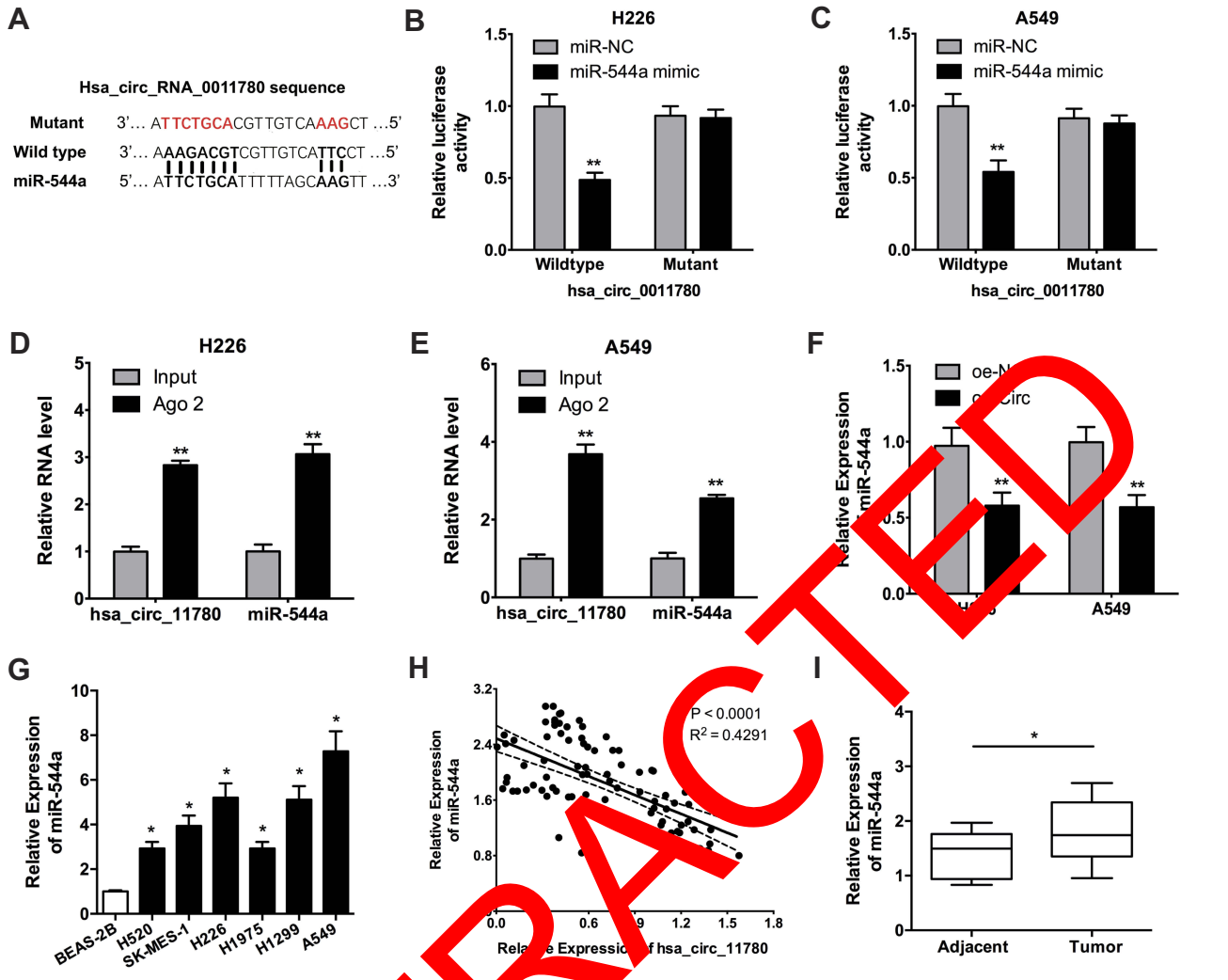

Figure 4 Hsa_circ_11780 modulates NSCLC gro[illegible] by targeting [illegible]544a. (**A**) The schematic diagram presents the complementary binding sites within hsa_circ_11780 and miR-544a. (**B, C**) Luciferase reporter assay confirmed the molecular binding between hsa_circ_11780 and miR-544a in H226 (**B**) and A549 (**C**). (**D, E**) The interaction between hsa_circ_11780 and miR-544a tested by RIP associated PCR in H226 (**D**) and A549 (**E**). (**F**) qPCR showed the miR-544a expression in NSCLC cells transfected with overexpressing vector or control. (**G**) MiR-544a expression in NSCLC cells (H226, H520, SK-MES-1, A549, H1975, and H1299) and BEAS-2B cells. (**H**) MiR-544a expression in NSCLC tissues and adjacent normal tissues shown by qPCR. (**I**) A negative correlation between the expression of hsa_circ_11780 and miR-544a in tumor tissues. $^{**}p < 0.01$, $^{*}p < 0.05$ compared to the control group.

tumor development. In a previous study, upregulated miR-544a was detected in metastatic tumor samples and cell lines of colorectal cancer.[22]

Homeobox A9 is vital for the regulatory role of miR-544a in migration and invasion.[22] The boosting function of miR-544a on migration and invasion of gastric cancer cells can be mediated by the degradation and the translocation of β-catenin by modulating the expression of cadherin 1 and Axis inhibition protein 2.[23] An investigation by Lu et al found that miR-544a could counteract cadherin 1 activity, leading to migration and invasion of breast cancer.[24] Our results represent a novel investigation of the important role of the circRNA-miR-544a-interaction in the tumorigenesis of NSCLC.

FBXW7, a tumor-suppressor gene, is a member of the F-box protein family.[25] Mutation and allelic loss of FBXW7 result in tumorigenesis in mice with increased FBXW7 and activated p53.[26] Inactivated FBXW7 often promotes malignant properties in various human cancers. FBXW7 in breast cancer, as an important component of E3 ubiquitin ligase, suppresses cell proliferation by mediating the ubiquitin-regulated degradation of Metadherin.[27] Targeting melanoma antigen A (MAGEA1), FBXW7 is involved in the ubiquitination and degradation of the Notch1 intracellular domain (NICD1), resulting in migration and proliferation of breast and ovarian cancercells.[28] Inactivation of FBXW7 in EGFR-TKI-sensitive cells

facilitates gefitinib resistance by strengthening epithelial-mesenchymal transition.[29] Increased fbxw7 and decreased skp2, switch stem cells from mitotic division to quiescence in lung adenocarcinoma, by regulating c-myc and p27.[30] miR-367 can maintain the stemness of lung carcinoma by activating the Wnt signal pathway through degradation of FBXW7.[31] Although FBXW7 is believed to be involved in tumor suppression and superior overall survival of patients with lung cancer,[32,33] few studies have investigated the regulatory upstream function of FBXW7 in NSCLC, particularly the circRNA-miRNA axis. Our study has shown that the hsa_circ_11780-miR-544a axis decreases the intracellular level of NSCLC cells (Figure 5). Collectively, our results suggest that FBXW7 acts as a modulator of the malignant properties of NSCLC cells in the circRNA-miRNA-interaction pathway.

In our study, miR-18a behaved as a functional connection between hsa_circ_11780 and FBXW7 expression.

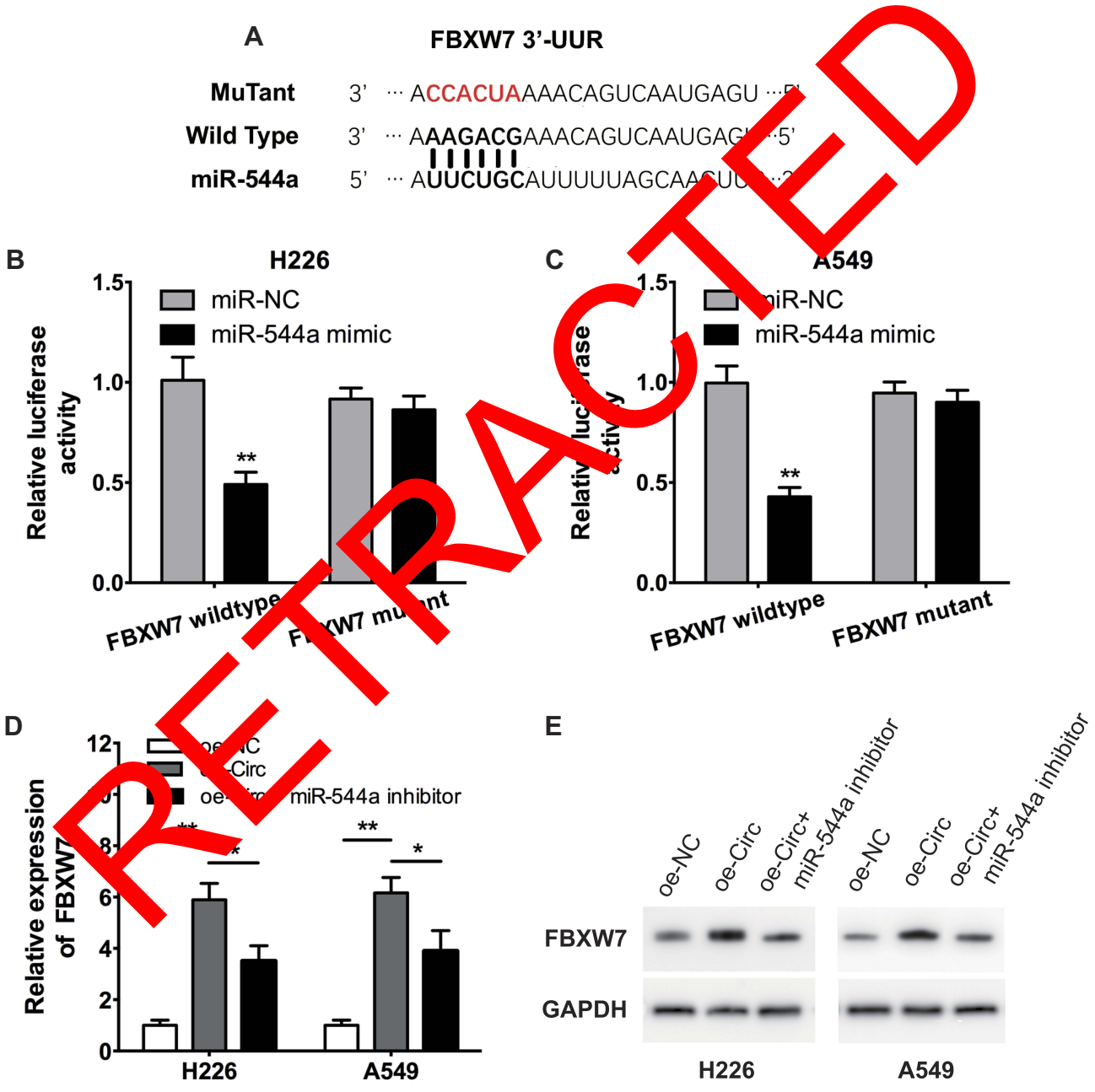

Figure 5 miR-544a directly targets FBWX7 in NSCLC development. (**A**) Bioinformatics tools reveal the complementary binding sites within miR-544a and FBWX7 3′-UTR. (**B, C**) Luciferase reporter assay validated the molecular binding between miR-544a and FBWX7 3′-UTR in H226 (**B**) and A549 (**C**). (**D, E**) Western blot assay showed the FBWX7 protein expression in NSCLC cells transfected with hsa_circ_11780 overexpressing vector or control. $^{**}p < 0.01$, $^{*}p < 0.05$ compared to the control group.

hsa_circ_11780 can mediate the expression of FBXW7 by post-transcriptional regulation. However, the specific molecular feedback from FBXW7 to hsa_circ_11780 has not been discussed in our study, and we recognize this as a limitation. An increasing number of reports state that interfering with the transcription of ncRNAs, by binding to their promotor regions, is the main feedback pattern of the downstream functional protein.[34–36] Zinc finger E-box binding homeobox 1 (ZEB1), which is downstream of the long noncoding RNA (lncRNA) ZEB1 antisense RNA 1(ZEB1-AS)/miR-409-3p, can activate the lncRNA ZEB1-AS expression by binding to its promoter region.[34] lncRNA CASC11 transcription was accelerated when the transcription factor FOXO3 translocated to the promoter of CASC11.[35] A similar positive feedback loop was found in the LINC01296/miR-598/Twist1 axis in NSCLC.[36] These findings indicate that FBXW7 or an FBXW7-related molecule may mediate the transcription of hsa_circ_11780 by functioning as a transcription factor in NSCLC. Nonetheless, this requires further exploration in future studies.

Conclusion

We have demonstrated that a low level of hsa_circ_00117[illegible] expression was associated with the large tumor size, advanced TMN stage, and inferior prognosis [illegible]CLC. Hsa_circ_0011780 can strongly inhibit th[illegible] prolife[illegible]tion, migration, and invasion of NSCLC in vitr[illegible] Furth[illegible] FBXW7 expression is mediated by hs[illegible]_circ_11[illegible] via complementary binding to miR-544a [illegible]CLC tumor[illegible]nesis. These data suggest that the hsa_circ_0[illegible]1780/miR-544a/FBXW7 axis may be a [illegible]omising therape[illegible]ic target for NSCLC.

Data Sha[illegible]ng Sta[illegible]m[illegible]nt

The dataset[illegible] analyze[illegible] during t[illegible]e current study are available from the [illegible]or[illegible]sponding [illegible]uthor on reasonable request.

Author Con[illegible]ibutions

Yong Liu, Chuanping Yang, Xin Jin, Chengsong Cao, and Qing Li contributed to the acquisition and analysis of data, drafting the article. Hanping Shi and Yong Liu contributed to the conception and design of this study, revising the manuscript. All authors contributed to data analysis, drafting and revising the article, gave final approval of the version to be published, and agree to be accountable for all aspects of the work.

Disclosure

The authors report no conflicts of interest in this work.

References

1. Bray F, Ferlay J, Soerjomataram I, Siegel RL, Torre LA, Jemal A. Global cancer statistics 2018: GLOBOCAN estimates of incidence and mortality worldwide for 36 cancers in 185 countries. *CA Cancer J Clin*. 2018;68(6):394–424. doi:10.3322/caac.v68.6
2. Perez-Moreno P, Brambilla E, Thomas R, Soria JC. Squamous cell carcinoma of the lung: molecular subtypes and therapeutic opportunities. *Clin Cancer Res*. 2012;18(9):2443–2451. doi:10.1158/1078-0432.CCR-11-2370
3. Crino L, Cappuzzo F. Present and fut[illegible] treat[illegible]t of advanced non-small cell lung cancer. *Semin O[illegible]l*. 2002;29(3 [illegible]ppl 9):9–16. doi:10.1053/sonc.2002.34266
4. Balata H, Fong KM, Hendriks L[illegible], et al. [illegible]evention an[illegible]early detection for NSCLC: advances [illegible] thoracic o[illegible]logy 2[illegible]8. *J Thorac Oncol*. 2019;14(9):1513–[illegible]27. doi:10[illegible]016/j.jt[illegible]9.06.011
5. Liu B, Ye B, Yang L, [illegible]al. Lo[illegible] noncoding RNA lncKdm2b is required for ILC3 [illegible]inte[illegible]y initiatio[illegible] of Zfp292 expression. *Nat Immunol*. 20[illegible];18(5):499–[illegible]8. doi:1[illegible]1038/ni.3712
6. Chen BJ, Byr[illegible] Takenaka K, [illegible]al. Analysis of the circular RNA transcripto[illegible]e in [illegible]ndometrial [illegible]ancer. *Oncotarget*. 2018;9(5):5786–5796. doi:10.[illegible]632/oncotarget.23534
7. Che[illegible], Yang L. Regu[illegible]on of circRNA biogenesis. *RNA Biol*. 2[illegible]5;12(4):381–388. doi:10.1080/15476286.2015.1020271
8. [illegible]lcheski FR, C[illegible]istoff AP, Margis R. Circular RNAs are miRNA s[illegible]nges and can [illegible] used as a new class of biomarker. *J Biotechnol*. 20[illegible]238:42–51. [illegible]oi:10.1016/j.jbiotec.2016.09.011
9. Chen [illegible], Zhu Y, et al. circPTN sponges miR-145-5p/miR-330-5p to promote proliferation and stemness in glioma. *J Exp Clin [illegible] Res*. 2019;38(1):398. doi:10.1186/s13046-019-1376-8
10. Yan L, Liu G, Cao H, Zhang H, Shao F. Hsa_circ_0035483 sponges hsa-miR-335 to promote the gemcitabine-resistance of human renal cancer cells by autophagy regulation. *Biochem Biophys Res Commun*. 2019;519(1):172–178. doi:10.1016/j.bbrc.2019.08.093
11. Ren S, Liu J, Feng Y, et al. Knockdown of circDENND4C inhibits glycolysis, migration and invasion by up-regulating miR-200b/c in breast cancer under hypoxia. *J Exp Clin Cancer Res*. 2019;38(1):388. doi:10.1186/s13046-019-1398-2
12. Chi Y, Luo Q, Song Y, et al. Circular RNA circPIP5K1A promotes non-small cell lung cancer proliferation and metastasis through miR-600/HIF-1alpha regulation. *J Cell Biochem*. 2019;120(11):19019–19030. doi:10.1002/jcb.29225
13. Wang Y, Li H, Lu H, Qin Y. Circular RNA SMARCA5 inhibits the proliferation, migration, and invasion of non-small cell lung cancer by miR-19b-3p/HOXA9 axis. *Onco Targets Ther*. 2019;12:7055–7065. doi:10.2147/OTT.S216320
14. Huang MS, Liu JY, Xia XB, et al. Hsa_circ_0001946 inhibits lung cancer progression and mediates cisplatin sensitivity in non-small cell lung cancer via the nucleotide excision repair signaling pathway. *Front Oncol*. 2019;9:508. doi:10.3389/fonc.2019.00508
15. Dong Y, He D, Peng Z, et al. Circular RNAs in cancer: an emerging key player. *J Hematol Oncol*. 2017;10(1):2. doi:10.1186/s13045-016-0370-2
16. Chen D, Ma W, Ke Z, Xie F. CircRNA hsa_circ_100395 regulates miR-1228/TCF21 pathway to inhibit lung cancer progression. *Cell Cycle*. 2018;17(16):2080–2090. doi:10.1080/15384101.2018.1515553
17. Lu C, Jiang W, Hui B, et al. The circ_0021977/miR-10b-5p/P21 and P53 regulatory axis suppresses proliferation, migration, and invasion in colorectal cancer. *J Cell Physiol*. 2019. doi:10.1002/jcp.29135
18. Xiaotong S, Jutong S, Hua H, Zhan Y, Haichao L. Hsa_circ_0070269 inhibits hepatocellular carcinoma progression through modulating miR-182/NPTX1 axis. *Biomed Pharmacother*. 2019;120:109497. doi:10.1016/j.biopha.2019.109497

19. Liang Y, Song X, Li Y, et al. circKDM4C suppresses tumor progression and attenuates doxorubicin resistance by regulating miR-548p/PBLD axis in breast cancer. *Oncogene*. 2019;38(42):6850–6866. doi:10.1038/s41388-019-0926-z
20. Li Z, Ruan Y, Zhang H, Shen Y, Li T, Xiao B. Tumour-suppressive circRNAs: mechanisms underlying their suppression of tumour occurrence and use as therapeutic targets. *Cancer Sci*. 2019. doi:10.1111/cas.14211
21. Wang H, Xiao Y, Wu L, Ma D. Comprehensive circular RNA profiling reveals the regulatory role of the circRNA-000911/miR-449a pathway in breast carcinogenesis. *Int J Oncol*. 2018;52(3):743–754. doi:10.3892/ijo.2018.4265
22. Sun S, Su C, Zhu Y, et al. MicroRNA-544a regulates migration and invasion in colorectal cancer cells via regulation of homeobox A10. *Dig Dis Sci*. 2016;61(9):2535–2544. doi:10.1007/s10620-016-4186-2
23. Yanaka Y, Muramatsu T, Uetake H, Kozaki K, Inazawa J. miR-544a induces epithelial-mesenchymal transition through the activation of WNT signaling pathway in gastric cancer. *Carcinogenesis*. 2015;36(11):1363–1371. doi:10.1093/carcin/bgv106
24. Lu P, Gu Y, Li L, Wang F, Qiu X. miR-544a promotes breast cancer cell migration and invasion reducing cadherin 1 expression. *Oncol Res*. 2016;23(4):165–170. doi:10.3727/096504016X14519157902726
25. Yeh CH, Bellon M, Nicot C. FBXW7: a critical tumor suppressor of human cancers. *Mol Cancer*. 2018;17(1):115. doi:10.1186/s12943-018-0857-2
26. Akhoondi S, Sun D, von der Lehr N, et al. FBXW7/hCDC4 is a general tumor suppressor in human cancer. *Cancer Res*. 2007;67(19):9006–9012. doi:10.1158/0008-5472.CAN-07-1320
27. Chen X, Li XY, Long M, et al. The FBXW7 tumor suppressor inhibits breast cancer proliferation and promotes apoptosis by targeting MTDH for degradation. *Neoplasma*. 2018;65(2):201–209. doi:10.4149/neo_2018_170228N149
28. Zhao J, Wang Y, Mu C, Xu Y, Sang J. MAGEA1 interacts with FBXW7 and regulates ubiquitin ligase-mediated turnover of NICD1 in breast and ovarian cancer cells. *Oncogene*. 2017;36(35):5023–5034. doi:10.1038/onc.2017.131
29. Xiao Y, Yin C, Wang Y, et al. FBXW7 deletion contributes to lung tumor development and confers resistance to gefitinib therapy. *Mol Oncol*. 2018;12(6):883–895. doi:10.1002/1878-0261.12200
30. Zhang W, Ren Z, Jia L, Li X, Jia X, Han Y. Fbxw7 and Skp2 regulate stem cell switch between quiescence and mitotic division in lung adenocarcinoma. *Biomed Res Int*. 2019;2019:9648269. doi:10.1155/2019/9648269
31. Xiao G, Zhang B, Meng J, et al. miR-367 stimulates Wnt cascade activation through degrading FBXW7 in NSCLC stem cells. *Cell Cycle*. 2017;16(24):2374–2385. doi:10.1080/15384101.2017.1380136
32. Liu X, Ma J, Xu F, Li L. TINCR suppr[illegible]proliferation and invasion through regulating miR-544a/FBX[illegible] axis i[illegible]ng cancer. *Biomed Pharmacother*. 2018;99:9–17. do[illegible].1016/j.biophi[illegible]2018.01.049
33. Chang H, Liu YH, Wang LL, et [illegible] MiR-182 prom[illegible]es cell proliferation by suppressing FBX[illegible]7 and F[illegible]XW11 in n[illegible]-small cell lung cancer. *Am J Transl R[illegible]* 2018;10(4):1[illegible]–1142
34. Qu R, Chen X, Zh[illegible]g C. Lnc[illegible]NA ZE[illegible]81/miR-409-3p/ZEB1 feedback loop is in[illegible]ved in[illegible]e progression of non-small cell lung cancer. *Bioch[illegible] Bio[illegible]Res Com[illegible]n*. 2018;507(1–4):450–456. doi:10.101[illegible]bbrc.2018.1[illegible]59
35. Yan R[illegible]Y, Lai B, Lin[illegible]en J. The positive feedback loop FOX[illegible]/CASC[illegible]/miR-498 promotes the tumorigenesis of non-small cell lung cance[illegible] *Biochem Biophys Res Commun*. 2019;519[illegible]:518–524. doi:10.1[illegible]6/j.bbrc.2019.08.136
36. Xu L, Wei B, Hui H, et al. Positive feedback loop of lncRNA LINC0129[illegible]iR-598/Twist1 promotes non-small cell lung cancer tumorigenes[illegible] *J Cell Physiol*. 2019;234(4):4563–4571. doi:10.1002/[illegible]cp.27235